noncontiguous 7-mm-thick slices (with 3.5-mm interslice gaps). In each functional sequence, eight test and eight control scans alternated for a total of 120 scans. In the test periods, the above hand identification task was given, with one trial every 2.6 s (Fig. 4i). The subjects were asked to report the handedness of each stimulus within 2.6 s by pressing either a head-side or foot-side key on the abdomen with the index fingers of both hands simultaneously. The stimulus disappeared upon response or at the end of the 2.6 s. In the control periods, the hand stimuli were replaced by scrambled hands (Fig. 4j). The subjects were asked to report whether the majority of the lines were near oblique or horizontal/vertical by key pressing. In the left-hand sequence, 81% (13/16) of the stimuli were left hands, and vice versa in the right-hand sequence. The subjects were tested under both new and old image instructions for both left and right hand sequences on days 34–38. A post-test was conducted five months after removal of the reversing spectacles. The post-test was equivalent to the old-image instruction because the subjects claimed that the new hand image did not make sense at that time.

All fMRI data were processed using the SPM99 software package (http://www.fil.ion.ucl.ac.uk). Standard linear image realignment, linear normalization to the stereotactic anatomical space and spatial smoothing (three-dimensional gaussian kernel, 4.7 mm full-width at half-maximum) were successively performed for each subject. Then, the data from subjects were pooled together and group comparisons were performed using the general linear model. Comparing hand identification with orientation judgement, significant increases were tested with t statistics and displayed as statistical parametric maps. Threshold for significance was set at voxel-level $P < 0.05$, corrected for multiple comparisons.

Received 22 May; accepted 14 July 2000.

1. Kohler, I. The formation and transformation of the perceptual world. *Psychol. Issues* **3** (monogr. 12) 1–173 (1964).
2. Stratton, G. M. Vision without inversion of the retinal image. *Psychol. Rev.* **4,** 341–360; 463–481 (1897).
3. Sugita, Y. Global plasticity in adult visual cortex following reversal of visual input. *Nature* **380,** 523–526 (1996).
4. Miyauchi, S. *et al.* Adaptation to reversing prisms activates the ipsilateral visual cortex in humans: an fMRI study. *Invest. Ophthalmol. Vis. Sci.* **40,** S820 (1999).
5. Held, R. Shifts in binaural localization after prolonged exposure to atypical combination of stimuli. *Am. J. Psychol.* **68,** 526–548 (1955).
6. Graziano, M. S. A., Yap, G. S. & Gross, C. G. Coding of visual space by premotor neurons. *Science* **266,** 1054–1057 (1994).
7. Sekiyama, K. Kinesthetic aspects of mental representations in the identification of left and right hands. *Percept. Psychophys.* **32,** 89–95 (1982).
8. Sekiyama, K. Mental and physical movements of hands: Kinesthetic information preserved in representational systems. *Jpn. Psychol. Res.* **25,** 95–102 (1983).
9. Bonda, E., Petrides, M., Frey, S. & Evans, A. Neural correlates of mental transformations of the body-in-space. *Proc. Natl Acad. Sci. USA* **92,** 11180–11184 (1995).
10. Parsons, L. M. *et al.* Use of implicit motor imagery for visual shape discrimination as revealed by PET. *Nature* **375,** 54–58 (1995).
11. Roland, P. E. *Brain Activation* (Wiley-Liss, New York, 1993).
12. Kosslyn, S. M., DiGirolamo, G. J., Thompson, W. L. & Alpert, N. M. Mental rotation of objects versus hands: neural mechanisms revealed by positron emission tomography. *Psychophysiology* **35,** 151–161 (1998).
13. Alivisatos, B. & Petrides, M. Functional activation of the human brain during mental rotation. *Neuropsychologia* **35,** 111–1118 (1997).
14. Jeannerod, M., Arbib, M. A., Rizzolatti, G. & Sakata, H. Grasping objects: the cortical mechanisms of visuomotor transformation. *Trends Neurosci.* **18,** 314–320 (1995).
15. Selemon, L. D. & Goldman-Rakic, P. S. Common cortical subcortical targets of the dorsolateral prefrontal and posterior parietal cortices in the rhesus monkey: Evidence for a distributed neural network subserving spatially guided behavior. *J. Neurosci.* **8,** 4049–4068 (1988).
16. Murray, E. A., Bussey, T. J. & Wise, S. P. Role of prefrontal cortex in a network for arbitrary visuomotor mapping. *Exp. Brain Res.* **1,** 114–129 (2000).
17. White, I. M. & Wise, S. P. Rule-dependent neuronal activity in the prefrontal cortex. *Exp. Brain Res.* **126,** 315–335 (1999).
18. Cohen, J. D. *et al.* Temporal dynamics of brain activation during a working memory task. *Nature* **386,** 604–608 (1997).
19. Courtney, S. M., Ungerleider, L. G., Keil, K. & Haxby, J. V. Transient and sustained activity in a distributed neural system for human working memory. *Nature* **386,** 608–611 (1997).
20. Perenin, M. T. & Vighetto, A. Optic ataxia: A specific disruption in visuomotor mechanisms. *Brain* **111,** 643–674 (1988).
21. Clower, D. M. *et al.* Role of posterior parietal cortex in the recalibration of visually guided reaching. *Nature* **383,** 618–621 (1996).
22. Snyder, L. H., Batista, A. P. & Andersen, R. A. Coding of intention in the posterior parietal cortex. *Nature* **386,** 167–170 (1997).
23. Rushworth, M. F. S., Nixon, P. D. & Passingham, R. E. Parietal cortex and movement: I. Movement selection and reaching. *Exp. Brain Res.* **117,** 292–310 (1997).
24. Taira, M., Mine, S., Georgopoulos, A. P., Murata, A. & Sakata, H. Parietal cortex neurons of the monkey related to the visual guidance of hand movement. *Exp. Brain Res.* **83,** 29–36 (1990).
25. Iriki, A., Tanaka, M. & Iwamura, Y. Coding of modified body schema during tool use by macaque postcentral neurons. *NeuroReport* **7,** 2325–2330 (1996).
26. Krams, M., Rushworth, M. F. S., Deiber, M. P., Frackowiak, R. S. J. & Passingham, R. E. The preparation, execution and suppression of copied movements in the human brain. *Exp. Brain Res.* **120,** 386–398 (1998).
27. Grafton, S. T., Arbib, M. A., Fadiga, L. & Rizzolatti, G. Localization of grasp representations in humans by positron emission tomography: 2. Observation compared with imagination. *Exp. Brain Res.* **112,** 103–111 (1996).
28. Rizzolatti, G., Fadiga, L., Gallese, V. & Fogassi, L. Premotor cortex and the recognition of motor actions. *Cogn. Brain Res.* **3,** 131–141 (1996).
29. Kurata, K. & Hoshi, E. Reacquisition deficits in prism adaptation after muscimol microinjection into the ventral premotor cortex of monkeys. *J. Neurophysiol.* **81,** 1927–1938 (1999).

Supplementary information is available on *Nature*'s World-Wide Web site (http://www.nature.com) or as paper copy from the London editorial office of *Nature*.

Acknowledgements

We thank M. Kato, T. Hayakawa, T. Murata, H. Tanabe and M. Nakatsuka for technical assistance and discussions.

Correspondence and requests for materials should be addressed to K.S. (e-mail: sekiyama@fun.ac.jp).

IRS-2 pathways integrate female reproduction and energy homeostasis

Deborah J. Burks*, Jaime Font de Mora†, Markus Schubert*, Dominic J. Withers‡, Martin G. Myers*, Heather H. Towery*, Shari L. Altamuro*, Carrie L. Flint* & Morris F. White*

* *Howard Hughes Medical Institute, Joslin Diabetes Center, Harvard Medical School, One Joslin Place, Boston, Massachusetts 02215, USA*
† *Centro de Investigacion del Cancer, Facultad de Medicina, Universidad de Salamanca, Salamanca 37007, Spain*

Severe dietary restriction, catabolic states and even short-term caloric deprivation impair fertility in mammals. Likewise, obesity is associated with infertile conditions such as polycystic ovary syndrome[1,2]. The reproductive status of lower organisms such as *Caenorhabditis elegans* is also modulated by availability of nutrients[3,4]. Thus, fertility requires the integration of reproductive and metabolic signals. Here we show that deletion of insulin receptor substrate-2 (IRS-2), a component of the insulin/insulin-like growth factor-1 signalling cascade, causes female infertility. Mice lacking IRS-2 have small, anovulatory ovaries with reduced numbers of follicles. Plasma concentrations of luteinizing hormone, prolactin and sex steroids are low in these animals. Pituitaries are decreased in size and contain reduced numbers of gonadotrophs. Females lacking IRS-2 have increased food intake and obesity, despite elevated levels of leptin. Our findings indicate that insulin, together with leptin and other neuropeptides, may modulate hypothalamic control of appetite and reproductive endocrinology. Coupled with findings on the role of insulin-signalling pathways in the regulation of fertility, metabolism and longevity in *C. elegans* and *Drosophila*[3–5], we have identified an evolutionarily conserved mechanism in mammals that regulates both reproduction and energy homeostasis.

Insulin receptor substrate (IRS) proteins undergo rapid tyrosine phosphorylation in response to insulin and insulin-like growth factor-1 (IGF-1). The mammalian IRS protein family contains at least four members: IRS-1 and IRS-2, which are widely expressed; IRS-3, which is found predominantly in adipose tissue; and IRS-4, which is expressed in the thymus, brain and kidney[6,7]. We have shown, using murine gene deletion, that IRS-2 is critical for peripheral carbohydrate metabolism and β-cell function[8,9]. In addition, IRS-1 mediates embryonic and post-natal somatic growth[8]. In *C. elegans*, the insulin/IGF-1 receptor homologue DAF-2 through the AGE-1 phosphatidylinositol-3-OH kinase (PI(3)K), regulates development, reproduction and longevity in response to environmental signals such as food[3]. Mutations in these pathways can induce developmental arrest at the dauer stage, reduce

‡ Present address: Department of Metabolic Medicine, Imperial College School of Medicine, Hammersmith Campus, DuCane Road, London W12 ONN, UK.

fertility and/or extend life-span[4,10]. Similarly, deletion of CHICO, the IRS protein of *Drosophila*, causes female sterility and reduced somatic growth and increased lipid storage[5].

During our analysis of the role of IRS-2 in carbohydrate metabolism[8], we found that matings between IRS-2$^{-/-}$ females and IRS-2$^{-/-}$ males did not yield a single pregnancy. To characterize the impaired reproduction, we established controlled breedings using various IRS genotypes (Fig. 1a). Only 9% of IRS-2$^{-/-}$ females (4–6-week-old virgins) that mated with wild-type males became pregnant during an 8-week period, and this was reduced to 0% when IRS-2$^{-/-}$ females were bred with IRS-2$^{-/-}$ males (Fig. 1a). IRS-2$^{-/-}$ males also displayed reduced fertility. If mated before the onset of severe diabetes, however, IRS-2$^{-/-}$ males were adequate breeders. Detailed analysis of our knockout colony revealed a sexual dimorphism in the diabetic phenotype: defects in carbohydrate metabolism imposed by deletion of IRS-2 were less severe in females than in males. Although IRS-2$^{-/-}$ males were severely glucose intolerant by 6 weeks, IRS-2$^{-/-}$ females displayed only slightly elevated blood glucose levels and mildly impaired glucose tolerance (Fig. 1b, c). IRS-2$^{-/-}$ females maintained fasting glucose levels in the range 120–160 mg dl^{-1} until about 4–5 months of age. All females used in the reproductive study were less than 10 weeks of age and so were relatively euglycaemic and mildly insulin resistant. It is therefore unlikely that the profound disturbance in fertility is a direct consequence of abnormal glucose metabolism in female IRS-2$^{-/-}$ animals.

We monitored IRS-2 matings daily for the presence of vaginal plugs—an indication of copulation and indirect evidence for lordotic behaviour. Copulation plugs were rarely noted in IRS-2$^{-/-}$ females during the course of this study (18.2% of IRS-2$^{-/-}$ compared with 100% of wild type). These observations suggest dysregulation of the oestrous cycle and normal sexual behaviour rather than failed implantation as the underlying cause of the infertility. Gross anatomical examination of 6-week-old IRS-2$^{-/-}$mice revealed normal development of the external genitalia and the reproductive tract; however, the ovaries of IRS-2$^{-/-}$ mice were small, contained very few surface follicles and displayed thickening of the cortex (Fig. 2a). Histological examination of ovarian sections from IRS-2$^{-/-}$ females revealed further evidence of anovulation including thickening of the ovarian stroma and an almost complete absence of corpora lutea (number of corpora lutea/ovary in wild type, 4.2 ± 0.6, $n = 9$; in IRS-2$^{-/-}$, 0.4 ± 0.2, $n = 12$) (Fig. 2b, c). Adult ovaries also contained decreased numbers of primary follicles with few growing follicles reaching an antral phase of development (Fig. 2c).

Quantitation of primary oocytes from embryos at day 18.5 revealed reduced numbers of these cells in the IRS-2$^{-/-}$ ovary as compared with wild-type controls (Fig. 2d), suggesting that the absence of IRS-2 impairs proliferation and/or increases apoptosis in this cell population during ovarian development. Notably, IGF-I and activation of PI(3)K have been identified as crucial mediators of germ-cell survival during murine embryonic oogenesis[11]. IRS-2 may therefore represent an important component of IGF-I and/or other developmental signalling pathways during fetal oogenesis. Both IRS-1 and IRS-2 were present in normal adult ovaries and phosphorylated during insulin stimulation (Fig. 2e). Expression and insulin-stimulated phosphorylation of IRS-1 in IRS-2$^{-/-}$ ovaries were comparable to levels detected in control animals (Fig. 2e), suggesting either that IRS-2 pathways transmit a specific function in this tissue or that normal development and endocrine regulation of ovarian physiology requires a signalling balance between IRS molecules.

To investigate further the defective reproduction in IRS-2$^{-/-}$ females, we measured sex steroid hormones and luteinizing hormone levels during stages of the oestrous cycle. Many IRS-2 knockouts (61%) failed to cycle but remained permanently in an inactive or dioestrous state. In both dioestrous and oestrous states, sex steroid hormones were reduced in IRS-2 knockouts (Fig. 3a). Normally, if ovarian feedback signals to the pituitary–hypothalamic axis are removed, as in the case of ovarian failure or ovariectomy, luteinizing hormone levels are elevated owing to loss of sex steroid suppression of gonadotropin-releasing hormone. Unexpectedly, luteinizing hormone levels were low in IRS-2$^{-/-}$ animals, suggesting that there are defects in production and/or release of this hormone. Elevated prolactin is commonly associated with human infertility and we therefore assayed circulating prolactin levels of IRS-2$^{-/-}$female mice. Consistent with observations regarding other reproductive

a

Cross	No. of pairs	% Pregnant
MWT x FWT	16	100
M2$^{-/-}$ x FWT	18	88.8
MWT x F2$^{-/-}$	22	9.0
M2$^{+/-}$ x F2$^{+/-}$	14	100
M2$^{-/-}$ x F2$^{-/-}$	20	0
M1$^{-/-}$ x FWT	12	100
F1$^{-/-}$ x MWT	16	68.8
M1$^{+/-}$ x F1$^{+/-}$	20	100
M1$^{-/-}$ x F1$^{-/-}$	14	64.2

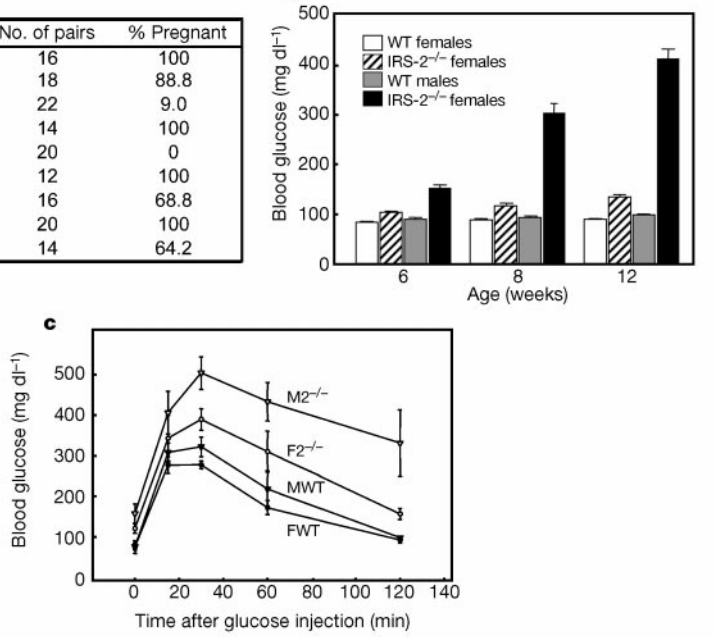

Figure 1 Reproductive and metabolic characteristics of IRS-2-deficient animals. **a**, Percentage of pregnancies. 4–6-week-old females were mated with experienced males of the indicated genotypes. Matings were monitored for pregnancies during an 8-week period. MWT, male wild-type; FWT, female wild-type; M2$^{-/-}$, male IRS-2 knockout; F2$^{-/-}$, female IRS-2 knockout; M1$^{-/-}$, male IRS-1 knockout; F1$^{-/-}$, female IRS-1 knockout. **b**, Blood glucose levels in 6-, 8-, and 12-week-old mice after a 15-h overnight fast. **c**, Glucose tolerance tests in fasted 6-week-old mice after intraperitoneal injection of 2 g D-glucose per kg body weight. Results in **b** and **c** are the mean ± s.e.m. of six mice of each genotype.

hormones, prolactin levels were reduced in these animals (wild-type, 10.6 ± 2.2 ng ml^{-1}, n = 5 mice; IRS-2$^{-/-}$, 6.6 ± 1.2 ng ml^{-1}, n = 8 mice). IRS-2$^{-/-}$ females were also resistant to exogenous gonadotropin stimulation: we retrieved only 0.25 ± 0.01 oocytes per animal (n = 8 animals) from the oviducts of superovulated IRS-2$^{-/-}$ mice, but 12 ± 0.8 oocytes per animal in wild-type controls (n = 6 animals).

The gene for IRS-2 has been implicated as being regulated by gonadal steroids[12]. As endogenous levels of oestrogen and progesterone are reduced in IRS-2 knockouts, we evaluated their response to exogenous sex steroids. Ovariectomized 6-week-old mice were treated for 3 weeks with a daily dose of 1 mg oestradiol or 1 μg progesterone, or a combination of both hormones. Uterine weight and morphology of treated knockouts were comparable to control values under all three experimental conditions, suggesting that uterine proliferation in IRS-2$^{-/-}$ females proceeded normally when regulated by exogenous steroids (Fig. 3b; data not shown). Oestradiol stimulates tyrosine phosphorylation of IRS-1 in uterine epithelial cells[13]. Short-term hormonal treatment (24 h) enhanced phosphorylation of IRS-1 in uterine extracts from IRS-2$^{-/-}$ females and controls (Fig. 3c). Moreover, hormonal induction of oestrogen receptor expression in IRS-2$^{-/-}$ tissue was similar to the levels detected in wild-type animals (Fig. 4c). These experiments show that tissues of the IRS-2 knockout respond appropriately to exogenous sex steroids.

To explore the potential defects of the reproductive axis that contributed to the low hormone levels, we analysed pituitary morphology in IRS-2$^{-/-}$ females. Pituitaries were reduced in size by roughly 30% (pituitary weight: wild-type, 45.6 ± 1.2 mg, n = 9; IRS-2$^{-/-}$, 31.4 ± 2.1 mg, n = 12) (Fig. 4a). Although pituitary size was globally diminished, disruption of IRS-2 particularly reduced the intermediate lobe, as visualized by immunostaining with anti-ACTH (adrenocorticotropic hormone) antibodies (Fig. 4a, b). To assess the effect of pituitary size reduction on endocrine function, we immunostained pituitary sections for growth hormone and the gonadotropins luteinizing hormone and follicle-stimulating hormone (FSH). The number of gonadotrophs was reduced by almost 40% in the IRS-2$^{-/-}$ pituitaries, whereas somatotrophs were equivalent between knockouts and wild-type animals (Fig. 4c). Reduction of the gonadotroph population implicates IRS-2 pathways in the development and maintenance of these hormone-producing cells and provides at least one explanation for the abnormal levels of luteinizing hormone and FSH in the IRS-2$^{-/-}$ females.

Many studies suggest that insulin serves as a link between the periphery and the brain at various levels of the neuroendocrine axis[14]. The receptors for insulin and IGF-1 show distinct patterns of expression within the pituitary gland; these receptors are detected on different subpopulations of secretory cells of the pars distalis[15,16]. Moreover, receptors for insulin are expressed by a subset of cells within the intermediate lobe[15]. To examine the capacity of IRS-2 to mediate insulin/IGF-1 signals in the neuroendocrine axis, we collected pituitaries after *in vivo* insulin stimulation of wild-type mice. Lysates of these glands were immunoprecipitated with either anti-IRS-1 or anti-IRS-2 antibodies and subsequently probed with anti-phosphotyrosine antibodies. Notably, there was tyrosine

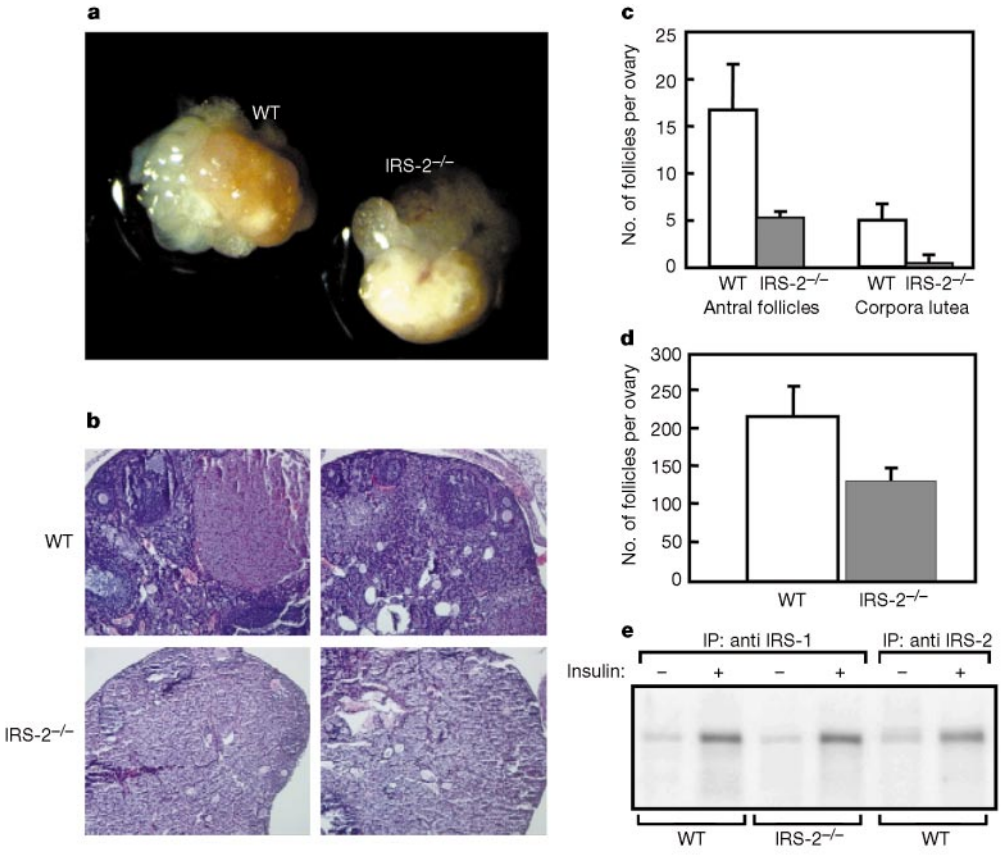

Figure 2 Ovarian phenotype of the IRS-2 knockout. **a**, Ovaries with attached oviducts and fallopian tubes from 8-week-old mice at ×2 magnification. **b**, Ovaries from 6–8-week-old mice. Sections were stained with haematoxylin and eosin and viewed at ×20 magnification. Representative ovarian sections are from two different animals of each genotype. **c**, Antral follicles (200–250 μm) and corpora lutea quantified from haematoxylin and eosin stained ovarian sections from 6–8-week-old mice viewed at ×20 magnification. Results are the mean ± s.e.m. of at least eight sets of ovaries from each genotype. **d**, Quantification of primary germ cells at embryo day 18. Fetal ovaries were collected and fixed in 4% paraformaldehyde. Primary oocytes were quantitated from haematoxylin and eosin stained sections of embryonic ovaries. Results are the mean ± s.e.m. of three females per genotype. **e**, Immunoblot of ovarian lysates. After *in vivo* insulin stimulation (5 units human insulin), ovaries were collected and homogenized. Lysates (1 mg total protein) were immunoprecipitated with anti-IRS antibodies as indicated, and immunocomplexes probed with anti-phosphotyrosine antibodies. Results are representative of three independent experiments.

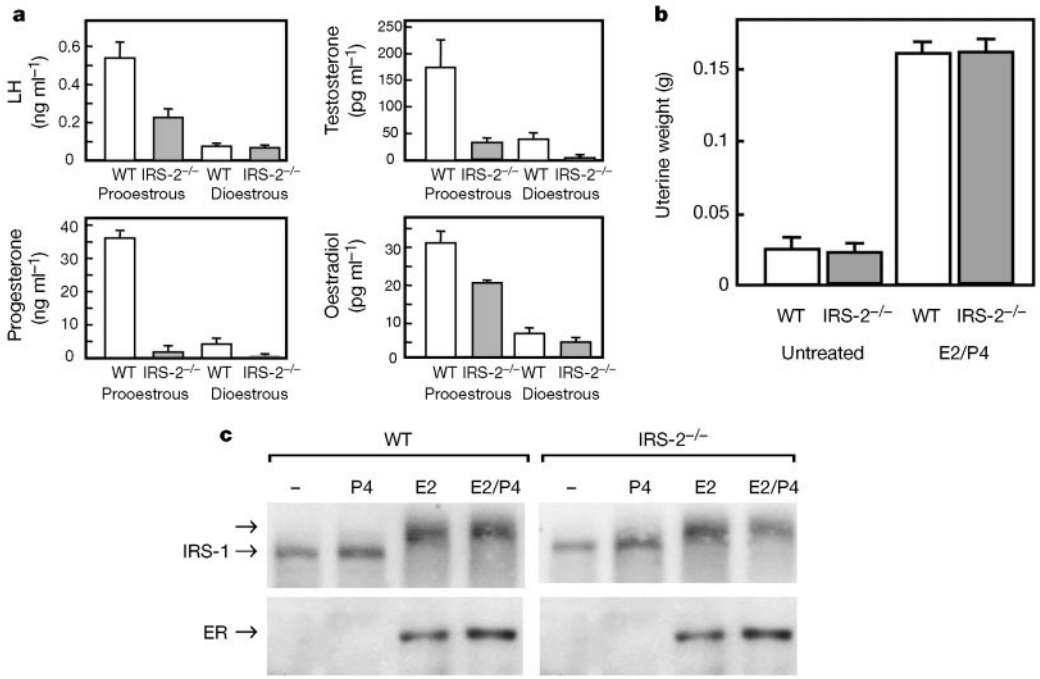

Figure 3 Reproductive hormone levels and response of ovariectomized mice to exogenous sex steroid stimulation. **a**, Plasma levels of reproductive hormones. Daily vaginal smears were used to assess the stage of the oestrous cycle. Serum was obtained from either pro-oestrous or dioestrous 8-week-old females by retro-orbital bleed. Wild-type pro-oestrous, $n = 6$; wild-type dioestrous, $n = 8$; IRS-$2^{-/-}$ pro-oestrous, $n = 6$; IRS-$2^{-/-}$ dioestrous, $n = 15$. **b**, Uterine weight. Ovaries were surgically removed from 6-week-old mice. Mice were allowed to recover for 2 weeks and then given daily subcutaneous doses of 1 mg oestradiol (E2) or 1 μg progesterone (P4), or both. Control animals were given vehicle mineral oil. After 21 days mice were killed, and uteri were dissected, cleared of fat and weighed to evaluate their proliferative response to sex steroid stimulation. Untreated animals, $n = 4$ females of each genotype; E2/P4 treated animals, $n = 6$ animals of each genotype. **c**, Immunoblots of uterine extracts. Lysates were immunoprecipitated for IRS-1, and immunoprecipitates were probed with anti-IRS-1 antibodies. E2 treatment reduced the mobility of IRS-1, indicative of enhanced phosphorylation. Total lysates (100 μg protein) were also probed for oestradiol-mediated induction of oestrogen receptor expression.

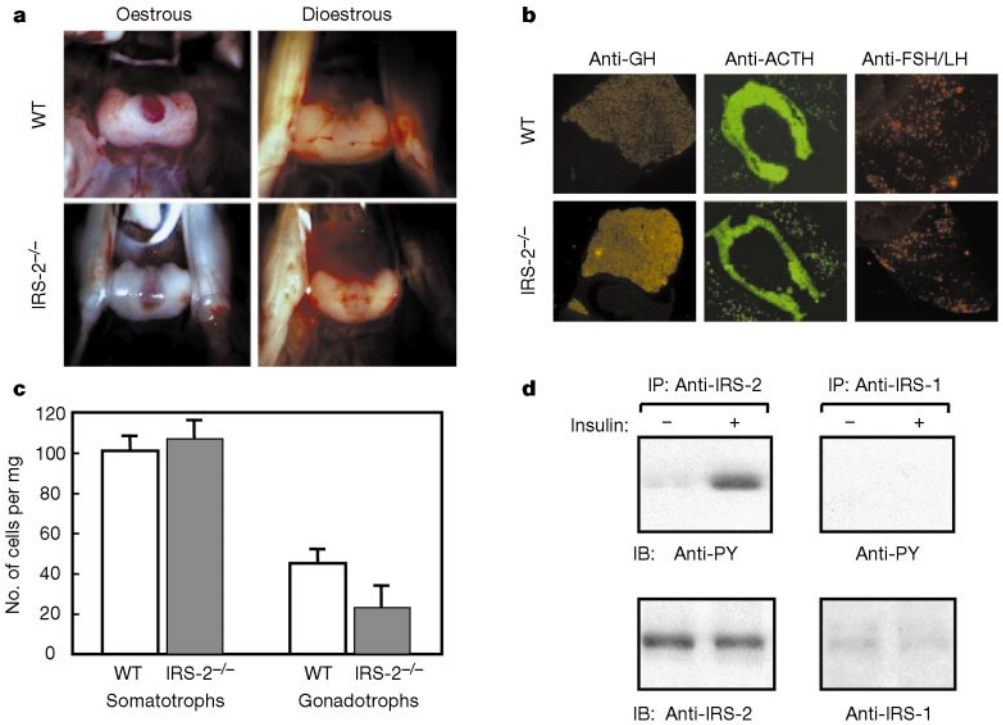

Figure 4 Pituitary phenotype of IRS-$2^{-/-}$ females. **a**, Representative pituitaries from oestrous and dioestrous 6–8-week-old females of each genotype at ×2 magnification. **b**, Immunofluorescent images of pituitary sections at ×20 magnification. Sections (1 μm) were co-immunostained for antibodies to growth hormone (GH), adrenocorticotropic hormone (ACTH), follicle stimulating hormone (FSH) and luteinizing hormone (LH). **c**, Quantitation of somatotrophs and gonadotrophs. Pituitary sections from 6–8-week-old females were co-immunostained for growth hormone, ACTH and FSH/LH. Results are mean ± s.e.m. of four mice from each genotype. **d**, Immunoblot of wild-type pituitary lysates after acute *in vivo* insulin stimulation (5 units, 10 min). Lysates (0.5 mg total protein) were immunoprecipitated with anti-IRS antibodies as indicated, and immunoprecipitates were probed with anti-phosphotyrosine antibodies. Pituitary lysates were pooled from three untreated or three insulin-stimulated mice. Results are representative of two independent experiments.

phosphorylation of IRS-2, but not of IRS-1 (Fig. 4d). Both molecules were present and tyrosine phosphorylated in liver lysates from these stimulated animals (data not shown). These results therefore suggest that IRS-2 pathways, based on either a distinct pattern of expression or a unique signalling capacity, may regulate normal development and function of the pituitary.

In *C. elegans* and *Drosophila*, homologues of the insulin/IGF-1/IRS signalling network have been implicated not only in the regulation of reproduction but also in the maintenance of fuel homeostasis[3–5]. In addition, insulin acts centrally to regulate appetite in mammals[14,17,18]. We therefore looked for evidence that IRS-2-dependent mechanisms might co-ordinate reproduction with energy balance. Monitoring of food intake showed that IRS-2$^{-/-}$ mice consumed 30% more chow than control animals (IRS-2$^{-/-}$, $4.5 \pm 0.30\,g\,day^{-1}$ per mouse; wild-type, $3.1 \pm 0.19\,g\,day^{-1}$ per mouse) (Fig. 5a). Furthermore, this increased food intake was reflected by abnormalities in fuel storage; IRS-2$^{-/-}$ mice weighed 20% more and stored two times more body fat than age-matched controls (Fig. 5b, c).

Circulating leptin levels were elevated more than 5-fold in the 8-week-old IRS-2$^{-/-}$ females as compared with controls, consistent with their increased adiposity (Fig. 5d). Moreover, leptin levels in IRS-2$^{-/-}$ females were elevated 2.5-fold (IRS-2$^{-/-}$, $6.1 \pm 0.8\,ng\,ml^{-1}$; wild-type, $2.4 \pm 0.4\,ng\,ml^{-1}$) as early as 4 weeks of age, before the onset of abnormal glucose tolerance. Leptin transmits critical signals regarding weight regulation to the central nervous system[14,19–21]. Genetic leptin resistance resulting from mutations in the murine leptin receptor (*db/db* mice) is associated with hyperphagia, weight gain and female infertility[22–24]. The elevated leptin levels and feeding abnormalities implicate leptin resistance as one explanation for the dysregulated energy homeostasis in IRS-2$^{-/-}$ females. We therefore assayed STAT3 phosphorylation in the hypothalamus of mice treated with an acute intravenous dose of leptin ($0.5\,\mu g\,g^{-1}$ body weight). Leptin receptor activation in the hypothalamus stimulates phosphorylation and nuclear translocation of STAT3; dysregulation of this pathway is associated with leptin resistance in *db/db* mice[25,26]. Hypothalamic lysates were immunoprecipitated with anti-STAT3 antibodies and immunocomplexes were subsequently probed with phosphospecific-STAT3 antibodies. Leptin stimulated phosphorylation of STAT3 in wild-type hypothalami (Fig. 5e); however, leptin-treated IRS-2$^{-/-}$ females displayed little or no activation of this pathway (Fig. 5e). Hypothalamic expression of STAT3 was equivalent between wild-type and knockout animals (Fig. 5e). These results show that IRS-2$^{-/-}$ females have hypothalamic resistance to leptin, and suggest that in the absence of IRS-2 pathways homeostatic mechanisms required for leptin sensing and/or signalling are impaired. Leptin has been reported to activate some components of the insulin signalling including IRS-1 and IRS-2 (refs 27–29), suggesting functional interactions between the insulin and leptin pathways.

Our results implicate IRS-2 pathways in the coordination of reproduction and energy homeostasis. Female IRS-2$^{-/-}$ mice have defects at more than one level of the hypothalamic–pituitary–ovarian axis, coupled with increased food intake and fat storage. IRS-2 may have evolved a unique role in this regulation, as IRS-1$^{-/-}$ mice do not present severe abnormalities in reproductive physiology (Fig. 1a; unpublished data). In addition to its classical metabolic effects, insulin, as well as IGF-1, may modulate ovarian function[1]. The IRS-2 model provides an important tool to unravel the complex pathogenesis of human infertility associated with insulin-resistant states such as polycystic ovarian syndrome[2]. Dysregulated IRS-2 expression or function may represent one underlying molecular defect responsible for these human endocrine disorders.

The feeding abnormalities of IRS-2$^{-/-}$ mice provide a molecular basis for the observation that intracerebroventricular administration of insulin decreases food intake in mammals[14,17]. Peripheral insulin resistance caused by deletion of IRS-2 (ref. 8) is probably accompanied by a loss of sensitivity to insulin in critical brain regions. Consistent with this hypothesis, obesity in IRS-2$^{-/-}$ mice occurs despite elevated leptin levels, suggesting that this hypothalamic leptin resistance is associated with both peripheral and central nervous system resistance to insulin action. Identification of

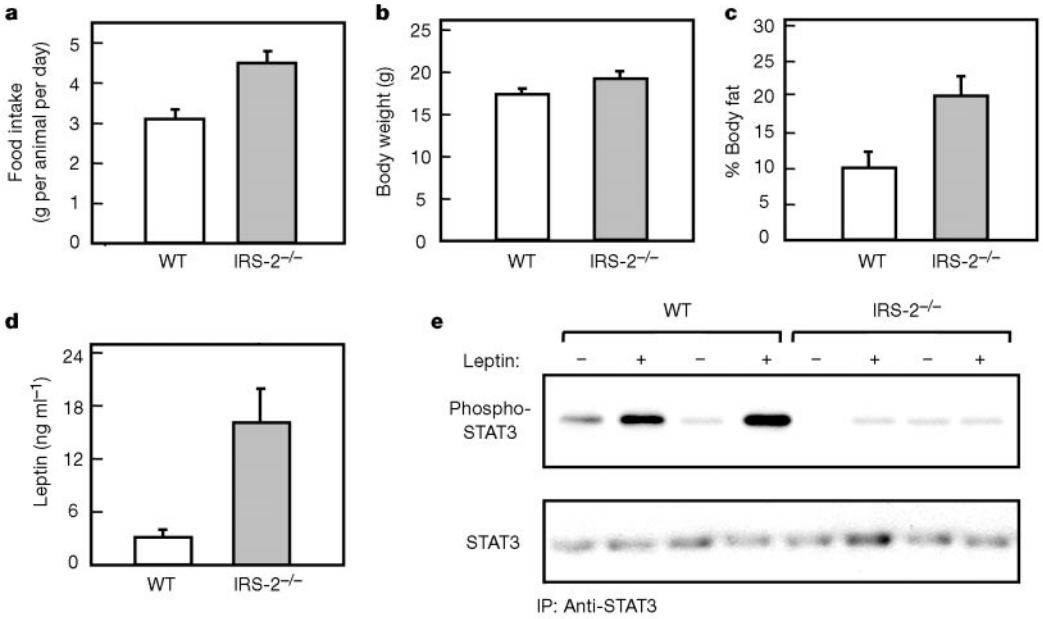

Figure 5 Analysis of feeding and energy homeostasis. **a**, Daily food intake. Female animals (6 weeks) were maintained on ground, normal mouse chow and monitored for 14 days. **b**, Body weight. Mice were weighed weekly from postnatal day 21 until 8 weeks of age. **c**, Body fat. Composition was determined by alkaline hydrolysis of carcasses and extraction of total lipids. **d**, Plasma leptin. Serum was collected by heart puncture and circulating leptin was measured by radioimmunoassay. Measurements were made on the same cohort of female mice in **a**–**d**; data are the mean ± s.e.m. of eight animals per genotype. **e**, Immunoblot of hypothalamic lysates. Eight-week-old mice were fasted overnight for 14–16 h. Anesthetized mice were then injected intravenously with a bolus of leptin ($0.5\,\mu g\,g^{-1}$ body weight). Untreated controls received an injection of saline. Two animals of each genotype were used for each condition. After 15 min, hypothalami were dissected and lysed. Lysates were immunoprecipitated with anti-STAT3 antibodies, and immunoprecipitates were then probed using phosphospecific STAT3 antibodies. Results represent two independent leptin stimulation experiments.

hypothalamic IRS-2 dependent signalling pathways will provide insights into the mechanisms of body weight regulation, and identify targets of therapeutic benefit. Our findings coupled with observations regarding insulin signalling pathways in *C. elegans* and *Drosophila* reveal an evolutionarily conserved mechanism by which neuroendocrine regulation of reproduction is coupled to appropriate energy metabolism. □

Methods

Mice

The generation of IRS-1 and IRS-2 knockout mice has been described[8,9]. Both mouse lines were maintained on a mixed C57Bl/6 × 129Sv genetic background. Genotyping of embryos and 3-week-old animals was done by Southern blotting as described[8]. Mice were maintained on normal light/dark cycle and handled in accordance with Joslin Diabetes Center Care and Use Committee protocols. Mating cages were monitored by 8:00 each day for the presence of vaginal plugs.

Hormone assays

To assess oestrous stages, we carried out daily vaginal smears. We collected blood for hormone assays by retro-orbital bleeds on anaesthetized mice or by tail bleeds. Murine luteinizing hormone and prolactin were measured by radioimmunoassay by T. Nett (Endocrine Laboratory of Colorado State University, Fort Collins). Sex steroids were assayed by the endocrine laboratory of the Brigham and Women's hospital and the laboratory of D. Hess (Oregon Regional Primate Center, Beaverton, OR). We determined leptin levels by radioimmunoassay using a mouse leptin standard (Linco).

Histology and immunostaining

We removed ovaries and uteri from adult animals and placed them in 10% buffered formalin. Tissues were embedded in paraffin, and 5-μm sections were prepared. Embryonic ovaries were collected in 4% paraformaldehyde. Pituitaries were fixed overnight in 4% paraformaldehyde and processed for electron microscopy. One-micron sections were stained with antibodies to growth hormone (Dako), and luteinizing hormone, FSH and ACTH, (A. F. Parlow, NIDDK, National Hormone and Pituitary Program). Detection was carried out using either rhodamine or fluoroscein antibodies (Jackson Immoresearch). For quantitation of ovarian follicles and pituitary cells, sections were viewed using a Zeiss Axiovert S100 microscope and video camera. Each section was covered systematically by accumulating non-overlapping fields of 1.5×10^6 μm^2. Counts and analysis were performed using Openlab image analysis software (Improvision Imaging).

Ovariectomy and sex steroid treatment

Ovariectomies were performed on 6-week-old virgins by veterinary services at Taconics Inc. Mice were allowed 2 weeks to recover from surgery. Subsequently, animals were given daily subcutaneous injections (100 μl) of 1 mg oestradiol or 1 μg progesterone, or a combination of both hormones for a period of 3 weeks. An immulsion of these hormones for injection was prepared in mineral oil. Control animals were injected daily with vehicle.

Superovulation and oocyte retrival

We induced 6-week-old virgins to ovulate by hormonal treatment. Animals were injected intraperitoneally with 10 units of pregnant mare horse serum (Boehringer-Mannheim) in sterile saline, and 35–40 h later with 15 units of human gonadotropic hormone (Sigma). We collected oocytes from oviducts the following morning.

In vivo hormone stimulations and immunoblotting

For *in vivo* stimulations with either insulin or leptin, animals were fasted overnight (14–16 h). After anesthesia with sodium amobarbital (100 mg kg^{-1}, intraperitoneal), a bolus of insulin (5 units regular human insulin) or leptin (0.5 μg g^{-1} body weight) was injected through the inferior vena cava. Controls received a comparable amount of diluent. Tissues (ovary, uterus and pituitary) were removed at times consitent with hormone action and homogenized at 4 °C as described[8]. Homogenates were allowed to solubilize for 1 h on ice and clarified by centrifugation at 16,000 *g* for 30 min. For detection of insulin-stimulated tyrosine phosphorylation, supernatants containing total protein (2 mg) were immunoprecipitated with an anti-IRS-1 or anti-IRS-2 antibodies[8]. Immunoblots were probed with anti-phosphotyrosine antibodies and detected by ^{125}I-protein A (ICN biochemicals). Blots were subsequently stripped and re-probed to reveal expression of IRS proteins. To assess activation of leptin pathways, we incubated hypthalamic lysates (0.5 mg) with antibodies to STAT3 (New England Biolabs) and then probed immunocomplexes with phosphospecific antibodies (New England Biolabs). For detection of the oestrogen receptor, 100 μg of tissue lysates was separated by SDS–PAGE and transferred to nitrocellulose. Membranes were probed with mouse monoclonal anti-ER antibodies (Neomarkers). Detection was by ^{125}-I protein A.

Metabolic measurements

Blood glucose levels were determined from mouse tails using a Glucometer Elite (Bayer). Glucose tolerance tests were carried out on mice after a 16-h fast as described[8].

Food intake and body composition analysis

Body weight was measured twice each week beginning on postnatal day 21. For measurement of food consumption, 6-week-old female mice were housed individually and food intake and body weight were assessed daily between 9:00 and 11:00 for a period of 14 days. Water and food were available *ad libitum*. Food consumption was deduced from the weight of chow remaining in wire-mesh feeding jars. Animals received a standard laboratory diet (Purina Mouse Chow) consisting of 6.5% (wt/wt) fat, 47% carbohydrates, and 23.5% protein. Animals were killed at 8 weeks of age and blood was obtained for metabolic measurements (leptin, insulin, triglycerides) by cardiac puncture. Carcasses were digested by alcoholic potassium hydroxide hydrolysis at 60 °C overnight and body lipid was analysed as described[30].

Received 11 April; accepted 14 June 2000.

1. Franks, S., Gilling-Smith, C., Watson, H. & Willis, D. Insulin action in the normal and polycystic ovary. *Endocrin. Metab. Clin. North Am.* **28,** 361–378 (1999).
2. Legro, R. S. *et al.* Phenotype and genotype in polycystic ovary syndrome. *Recent Prog. Horm. Res.* **53,** 217–256 (1998).
3. Tissenbaum, H. A. & Ruvkun, G. An insulin-like signaling pathway affects both longevity and reproduction in *Caenorhabditis elegans*. *Genetics* **148,** 703–717 (1998).
4. Hsin, H. & Kenyon, C. Signals from the reproductive system regulate the lifespan of *C. elegans*. *Nature* **399,** 362–366 (1999).
5. Bohni, R. *et al.* Autonomous control of cell and organ size by CHICO, a drosophila homolog of vertegrate IRS1-4. *Cell* **97,** 865–875 (1999).
6. Lavan, B. E., Lane, W. S. & Lienhard, G. E. The 60-kDa phosphotyrosine protein in insulin-treated adipocytes is a new member of the insulin receptor substrate family. *J. Biol. Chem.* **272,** 11439–11443 (1997).
7. Lavan, B. E. *et al.* A novel 160 kDa phosphotyrosine protein in insulin-treated embryonic kidney cells is a new member of the insulin receptor substrate family. *J. Biol. Chem.* **272,** 21403–21407 (1997).
8. Withers, D. J. *et al.* Disruption of IRS-2 causes type 2 diabetes in mice. *Nature* **391,** 900–904 (1998).
9. Withers, D. J. *et al.* Irs-2 coordinates Igf-1 receptor-mediated beta-cell development and peripheral insulin signalling. *Nature Genet.* **23,** 32–40 (1999).
10. Ogg, S. *et al.* The Fork head transcription factor DAF-16 transduces insulin-like metabolic and longevity signals in *C. elegans*. *Nature* **389,** 994–999 (1997).
11. Morita, Y. *et al.* Requirement for phosphatidylinositol-3-kinase in cytokine-mediated germ CEll survival during fetal oogenesis in the mouse. *Endocrinology* **140,** 941–949 (1999).
12. Vassen, L., Wegrzyn, W. & Klein-Hitpass, L. Human insulin receptor substrate-2 (IRS-2) is a primary progesterone response gene. *Mol. Endocrinol.* **13,** 485–494 (1999).
13. Richards, R. G., DiAugustine, R. P., Petrusz, P., Clark, G. C. & Sebastian, J. Estradiol stimulates tyrosine phosphorylation of the insulin-like growth factor-1 receptor and insulin receptor substrate-1 in the uterus. *Proc. Natl Acad. Sci. USA* **93,** 12002–12007 (1996).
14. Schwartz, M. W., Baskin, D. G., Kaiyala, K. J. & Woods, S. C. Model of the regulation of energy balance and adiposity by the central nervous system. *Am. J. Clin. Nutr.* **69,** 584–596 (1999).
15. Unger, J. W. & Betz, M. Insulin receptors and signal transduction proteins in the hypothalamo–hypophyseal system: a review on morphological findings and functional implications. *Histol. Histopathol.* **13,** 1215–1224 (1998).
16. Unger, J. W. & Lange, W. Insulin receptors in the pituitary gland: morphological evidence for influence on opioid peptide-synthesizing cells. *Cell Tissue Res.* **288,** 471–483 (1997).
17. Woods, S. C., Stein, L. J., McKay, L. D. & Porte, D. Chronic intracerebroventricular infusion of insulin reduces food intake and body weight of baboons. *Nature* **282,** 503–505 (1979).
18. Foster, L. A., Ames, N. K. & Emery, R. S. Food intake and serum insulin responses to intraventricular infusions of insulin and IGF-1. *Physiol. Behav.* **50,** 745–749 (1991).
19. Flier, J. S. What's in a name? In search of leptin's physiological role. *J. Clin. Endocrin. Metab.* **83,** 1407–1413 (1998).
20. Schwartz, M. & Seeley, R. Neuroendocrine responses to starvation and weight loss. *New Engl. J. Med.* **336,** 1802–18011 (1997).
21. Ahima, R., Prabakaran, D., Mantzoros, C. *et al.* Role of leptin in the neuroendocrine response to fasting. *Nature* **382,** 250–252 (1996).
22. Chehab, F. F., Lim, M. E. & Lu, R. Correction of the sterility defect in homozygous obese female mice by treatment with the human recombinant leptin. *Nature Genet.* **12,** 318–320 (1996).
23. Chen, H. *et al.* Evidence that the diabetes gene encodes the leptin receptor: Identification of a mutatioan in the leptin receptor gene in db/db mice. *Cell* **84,** 491–495 (1996).
24. Lee, G. H. *et al.* Abnormal splicing of the leptin receptor in *diabetic* mice. *Nature* **379,** 632–635 (1996).
25. Vaisse, C. *et al.* Leptin activation of Stat3 in the hypothalamus of wild-type and *ob/ob* mice but not *db/db* mice. *Nature Genet.* **14,** 95–97 (1996).
26. McCowen, K. C., Chow, J. C. & Smith, R. J. Leptin signaling in the hypothalamus of normal rats in vivo. *Endocrinology* **139,** 4442–4447 (1998).
27. Szanto, I. & Kahn, C. R. Selective interaction between leptin and insulin signaling pathways in a hepatic cell line. *Proc. Natl Acad. Sci* **97,** 2355–2360 (2000).
28. Berti, L., Kellerer, M., Capp, E. & Haring, H. U. Leptin stimluates glucose transport and glycogen synthesis in C2C23 myotubes: evidence for a PI 3-kinase mediated effect. *Diabetologia* **40,** 606–609 (1997).
29. Cohen, B., Novick, D. & Rubinstein, M. Modulation of insulin activities by leptin. *Science* **274,** 1185–1188 (1996).
30. Fredrich, R. C. *et al.* Leptin levels reflect body lipid content in mice: evidence for diet-induced resistance to leptin action. *Nature Med.* **1,** 1311–1314 (1995).

Acknowledgements

We are grateful to C. Cahill for preparation of pituitary sections; A. Parlow for antibodies to pituitary hormones; A. Dunaif for testosterone measurements; and D. Hess for helpful discussions of murine sex hormones.

Correspondence and requests for materials should be addressed to M.F.W. (e-mail: morris.white@joslin.harvard.edu).